

## Addressing and sustaining in alternating current coplanar plasma display panels

C. Punset, S. Cany, and J.-P. Boeuf<sup>a)</sup>

*Centre de Physique des Plasmas et Applications de Toulouse, Université Paul Sabatier,  
118 Route de Narbonne, 31062 Toulouse Cedex France*

(Received 23 November 1998; accepted for publication 23 March 1999)

In a coplanar plasma display panel the discharges in each pixel are sustained between two parallel electrodes on the same substrate. A third electrode perpendicular to the sustaining electrodes and placed on a facing substrate is used to address the pixel. A self-consistent two-dimensional model of the microdischarge has been used to simulate and study the addressing and sustaining phases in an alternating current coplanar cell. The formation and decay of the transient plasma during the address and sustain discharge pulses are described. The time evolution of the charges on the dielectric surfaces above each electrode is also discussed and the model is used to derive the voltage margins of the address and sustain regimes. © 1999 American Institute of Physics.

[S0021-8979(99)02113-1]

### I. INTRODUCTION

Plasma display panels (PDPs) are flat displays in which each picture element consists of microdischarges emitting VUV photons which are converted into visible (red, green, blue) by phosphors deposited on the discharge walls. The industrial production of PDPs for large area wall hanging televisions has recently started. However research is still needed to lower the power consumption and to improve the luminous efficiency and the contrast ratio of these displays. Numerical models of PDP discharge cells have been developed over the last few years and can help guide the optimization of these devices.<sup>1-4</sup>

Most companies are now developing alternating current (ac) PDPs where the electrodes are covered with a dielectric layer forming a capacitor in series with the discharge gap. A high frequency (typically 100 kHz) square-wave voltage is applied between the discharge electrodes, and the "ON state" of a discharge cell is characterized by a succession of transient discharge pulses. The amplitude of the electrode voltage during the sustain regime is below the gas breakdown voltage and an initial "write" voltage pulse is used to initiate a sequence of discharges.

Two different types of electrode geometry are used: the matrix (or double substrate) geometry and the coplanar (or single substrate) geometry. In both cases the discharges are confined between two parallel glass plates separated by a gas gap of about 100  $\mu\text{m}$ . The gas mixture contains a few percent of xenon [ultraviolet (UV) emitter] in neon or helium (to lower the breakdown voltage). In the matrix geometry the discharges are created at the intersections of column electrodes and row electrodes deposited on two parallel glass plates. The sustaining, square-wave voltage is applied continuously between the row and column electrodes and a specific cell is addressed by superimposing an "address" volt-

age pulse on the "sustain" voltage. The charges ("memory charges") on the dielectric surfaces at the end of the address pulse induce a voltage which adds to the sustain voltage at the next half cycle and the voltage across the gap can therefore become larger than the breakdown voltage. To successfully put a cell in the ON state, the address voltage must be larger than a minimum value which will be called the firing voltage in the following. The sequence of discharge pulses initiated by the address pulse can be stopped by applying to the cell electrodes a voltage whose amplitude is chosen in such a way that the memory charges are cancelled. The addressing of a matrix display is relatively simple and well understood<sup>1,3</sup> although work is still continuing to optimize the power consumption and UV efficiency. In a coplanar display, the sustain discharges occur between two parallel electrodes deposited on the same glass plate. A given cell is selected by using a third electrode (address electrode or data electrode) perpendicular to the coplanar electrodes and deposited on the facing glass plate. A discharge cell in a coplanar cell is therefore characterized by three electrodes (instead of two as in the matrix case). Although the principle of the addressing sequence in a coplanar display is the same as in the matrix case, there is a larger variety of possible addressing sequences and the presence of three electrodes makes the analysis of the addressing method more complicated.<sup>5-8</sup>

The purpose of this article is to study the discharge formation and decay and the addressing sequence in a coplanar PDP cell with the help, of a two-dimensional (2D) discharge model. The discharge model is similar to the one used by Punset, Boeuf, and Pitchford<sup>1</sup> for the modeling of a matrix cell. We briefly describe the principles of this model in Sec. II. The discharge formation and decay during the address pulse (or write, or "data" pulse) and the first sustain pulse in typical conditions is shown in Sec. III. The driving scheme used to describe the writing and sustaining in Sec. III is simplified for clarity. In Sec. IV we describe one of the possible driving methods used in actual PDPs. Section V gives a

<sup>a)</sup>Electronic mail: jpb@cpa01.ups.tlse.fr

short description of other possible driving schemes for coplanar cells. In this article we focus on addressing and sustaining, and we do not discuss the operation of erasing a cell.

## II. PHYSICAL AND NUMERICAL MODEL OF AN ac COPLANAR PDP CELL

The physical model used in this article is identical to the one described in Refs. 1 and 2. We therefore give below only a short description of this model.

### A. Physical model

The electrical model consists of the first two moment equations for electron and ion transport coupled with Poisson's equation for the electric field and with appropriate boundary conditions. The ionization coefficient is supposed to depend on the local electric field. This is a sufficient approximation for our purpose (see Ref. 2). The continuity equations and the momentum transfer equations in the drift-diffusion approximation for electrons and positive ions are written as

$$\frac{\partial n_e}{\partial t} + \nabla \cdot (n_e \bar{\mathbf{v}}_e) = S_e, \quad (1)$$

$$n_e \bar{\mathbf{v}}_e = n_e \mu_e \nabla V - D_e \nabla n_e, \quad (2)$$

$$\frac{\partial n_p}{\partial t} + \nabla \cdot (n_p \bar{\mathbf{v}}_p) = S_p, \quad (3)$$

$$n_p \bar{\mathbf{v}}_p = -n_p \mu_p \nabla V - D_p \nabla n_p, \quad (4)$$

where  $n_e$  is the electron density,  $n_p$  the positive ion density. As in Ref. 1, only two different types of ions,  $\text{Xe}^+$ , and  $\text{Ne}^+$  (the index  $p$  in the equations refers to xenon or neon ions) are considered.  $\bar{\mathbf{v}}_e$  and  $\bar{\mathbf{v}}_p$  represent the mean velocity for electrons and ions, respectively.  $S_e(\mathbf{r}, t)$  and  $S_p(\mathbf{r}, t)$  are the production rates for electrons and ions. The mobilities  $\mu_e$  and  $\mu_p$  are functions of the reduced electric field  $E/p$ . The  $D/\mu$  are set to constant values corresponding to an electron temperature of 1 eV and an ion temperature equal to the gas temperature.

The electron ionization source term  $S_e$  is expressed as

$$S_e(\mathbf{r}, t) = \alpha(\mathbf{r}, t) |\varphi_e(\mathbf{r}, t)|, \quad (5)$$

where  $\varphi_e = n_e \bar{\mathbf{v}}_e$  is the electron flux and  $\alpha$  the total ionization coefficient. The functional dependence of the ionization coefficient on the local electric field is supposed to be of the form

$$\alpha(\mathbf{r}, t) \equiv \alpha_{\text{swarm}} \left( \frac{\tilde{E}(\mathbf{r}, t)}{p} \right), \quad (6)$$

where  $\alpha_{\text{swarm}}$  is the ionization coefficient derived from a Boltzmann simulation with a constant field  $\tilde{E}$ ,  $p$  is the gas pressure, and  $\tilde{E}$  is related to the local field  $\mathbf{E}$  by

$$\begin{aligned} \tilde{E} &= \frac{-\mathbf{E} \cdot \varphi_e}{|\varphi_e|}, \quad \text{when } -\mathbf{E} \cdot \varphi_e > 0, \\ \tilde{E} &= 0 \quad \text{when } -\mathbf{E} \cdot \varphi_e \leq 0. \end{aligned} \quad (7)$$

The ionization source terms  $S_p$  for the positive ions are similar to  $S_e$  except that the total ionization coefficient must be replaced by the partial (xenon or neon) ionization coefficient.

Equations (1)–(4) above are coupled to Poisson's equation

$$\nabla \cdot [\epsilon \nabla V] = -e[n_p - n_e], \quad (8)$$

where  $\epsilon$  is the permittivity.

### B. Brief description of the numerical method

The equations above are solved for a 2D Cartesian geometry. The continuity equations are solved using a Cranck–Nicholson scheme with a Scharfetter–Gummel<sup>9</sup> exponential representation of the charged particle fluxes as in Punset, Boeuf, Pitchford.<sup>1</sup> Poisson's equation is solved with a successive overrelaxation method (SOR). In Ref. 1 the time integration of the transport equation and Poisson's equation is explicit, i.e., the electric field is taken at time  $t$  when the continuity equations are integrated between  $t$  and  $(t + \Delta t)$ . In this article the time integration is semi-implicit, as in Ref. 10. The electric field in the integration of the continuity equation between  $t$  and  $(t + \Delta t)$  is not the field at time  $t$ , but rather a prediction of the field at time  $(t + \Delta t)$ . The principle of the semi-implicit integration is summarized below. Poisson's equation is written as

$$\nabla \cdot [\epsilon \nabla V^{k+1}] = -e \left[ (n_p^k - n_e^k) + \Delta t \frac{\partial (n_p - n_e)}{\partial t} \right], \quad (9)$$

where the index ( $k$ ) refers to time ( $t^k$ ) and  $(k+1)$  corresponds to  $(t^{k+1} = t^k + \Delta t)$ . The second term in the right hand side of Eq. (9) corresponds to a correction of the charge density due to the variation of the electric field between  $t^k$  and  $t^{k+1}$ . Using the continuity Eqs. (1), (3), and the drift-diffusion Eqs. (2), (4), the time derivative in the right hand side of Eq. (9) is written as

$$\begin{aligned} -e \Delta t \frac{\partial (n_p - n_e)}{\partial t} &= -e \Delta t \nabla \cdot [(n_e^k \mu_e^k + n_p^k \mu_p^k) \nabla V^{k+1} \\ &\quad - (D_e^k \nabla n_e^k - D_p^k \nabla n_p^k)]. \end{aligned} \quad (10)$$

The charged particle fluxes in Eq. (10) above are discretized using the Scharfetter–Gummel scheme and linearized assuming a small variation of the potential between  $t^k$  and  $t^{k+1}$ . After putting the terms depending on  $V^{k+1}$  on the left hand side of Eq. (9) one obtains a modified Poisson's equation which can be solved with a SOR method.

This semi-implicit technique is stable for time steps much larger than the dielectric relaxation time  $\tau_r$  defined by

$$\tau_r = \frac{\epsilon_0}{e} \frac{1}{(n_e \mu_e + n_p \mu_p)},$$

and which is the maximum time step in an explicit method. We found that the method was stable and accurate for time steps as large as 50 times the dielectric relaxation time. In the calculations presented below we used time steps smaller than 25 times the dielectric relaxation time. The computation time

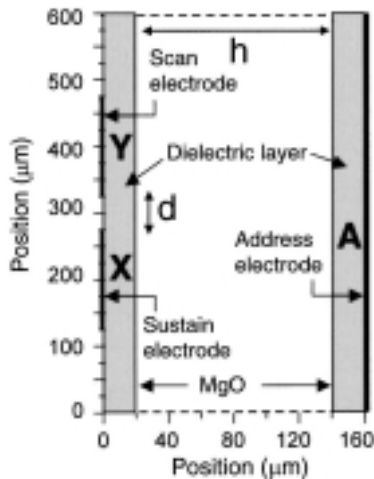


FIG. 1. Schematic of a coplanar ac PDP cell. Simulation domain. The A electrode is called the data or address electrode. The X and Y coplanar electrodes are called the display electrodes. X is sometimes called the sustain electrode (all the X electrodes have the same voltage). Y is called the scan electrode because during addressing a scan voltage pulse is applied successively to all the Y electrodes. If a large enough voltage is applied to the data electrode at the time the Y electrode receives the scan voltage pulse the (X-Y-A) cell is addressed. During sustaining the discharges occur between X and Y.

for the simulation of a  $5 \mu\text{s}$  discharge pulse at 500 Torr was on the order of 5 min on a PC Pentium 300 MHz.

### C. Geometry and boundary conditions

The typical geometry used for a coplanar cell simulation is shown in Fig. 1. The simulation domain is a rectangle. Symmetric or periodic boundary conditions can be used on the sides of the simulation domain perpendicular to the electrodes (periodic boundary conditions are used in the results presented in this article). On the side of the simulation domain in the plane of the coplanar electrodes (interface between dielectric layer and glass plate, left side of Fig. 1) the potential is set to the electrode voltages where electrodes are present. Between electrodes on the same side, the perpendicular electric field is set to zero. This condition implies, as in Punset, Boeuf, and Pitchford<sup>1</sup> that no current flows out of the simulated domain. The surface of the dielectric layers above the electrodes is covered with a thin layer of MgO which is used both to protect the dielectric layers and to lower the breakdown voltage (the secondary electron emission under bombardment of MgO by neon ions is large).

Dielectric barrier ribs separate the column electrodes in PDPs. However, these do not appear in the simulation domain since they are parallel to the data electrode and the model is only 2D.

The data or address electrode used to trigger the discharges between the coplanar electrodes is noted A in Fig. 1. The coplanar electrodes are noted X and Y. The X electrode is called the sustain electrode, and all the X electrodes along a given address electrode A are at the same potential. The Y electrode is the scan electrode. During addressing a voltage is applied between the scan electrode and the data electrode. During sustaining the successive discharges form between the X and Y electrodes due to the square wave, sustaining

voltage applied between them (frequency on the order of 100 kHz).

### D. Excited species kinetics

We do not discuss in this article the excited species kinetics and the photon emission. As has been shown in Refs. 2 and 11 the excited species model can be decoupled from the electric model of the discharge in typical PDP conditions because of the rather low energy density dissipated by electrons in the cell at each discharge pulse. The density of excited species in the discharge is not large enough for stepwise excitation or ionization processes to strongly influence the time evolution of the plasma density and electric field in the discharge. On the other hand, electron-ion recombination has not been included in the model. Recombination plays an important role in the afterglow after the discharge pulse since the plasma decay is controlled by recombination and ambipolar diffusion. The consequences of this approximation have been discussed in Ref. 11. We have checked that the results discussed in this article (power dissipation into xenon excitation, driving methods, margins) are not strongly affected by the decay time of the plasma during the afterglow.

## III. PLASMA FORMATION DURING THE ADDRESS AND SUSTAIN PULSES

The results presented in Sec. III correspond to a xenon-neon mixture with 5% xenon. The secondary emission coefficients for neon and xenon ions on MgO are taken to be 0.5 and 0.01, respectively. The gas pressure is 500 Torr. The width of the cell is  $600 \mu\text{m}$ , the gas gap length  $h$  is  $120 \mu\text{m}$ , and the dielectric layer thickness is set to  $20 \mu\text{m}$  (see Fig. 1). The relative permittivity of the dielectric is 10 unless otherwise indicated. The coplanar electrode gap length  $d$  is  $50 \mu\text{m}$ . The chosen values of these parameters are not optimized but they are typical of a 21 in. diagonal PDP.

### A. Simplified driving method used in this section and some definitions

In Sec. III A we consider the addressing sequence represented in Fig. 2.

A voltage pulse is applied between the Y electrode (see Fig. 1) and the A electrode and a discharge is initiated between the two facing electrodes Y and A. The X electrode voltage is set to zero during this address pulse, and the voltages applied to Y and A will be called “scan write” and data voltages, respectively. A succession of sustain voltage pulses is then applied between the X and Y electrodes. The voltage of the address electrode is set to zero during the sustain regime. We describe the plasma formation during the address pulse and the first sustain pulse in Secs. III B and III C, respectively. The charge evolution on the dielectric surface above the electrodes is shown in Sec. III D. In practice the sustain regime often starts after all the cells have been addressed. This method is called address display period sepa-

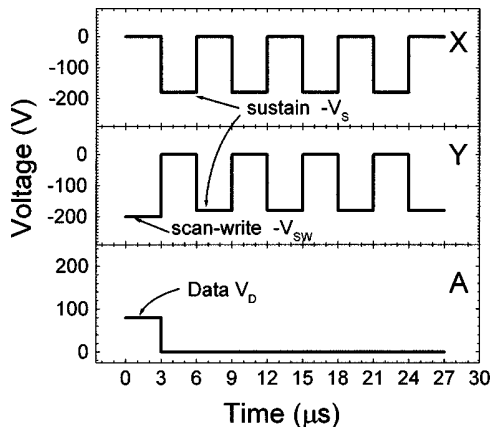


FIG. 2. Voltages applied to the electrodes to simulate an address (also called data pulse) discharge between Y and A, and several sustain pulses (discharges between X and Y). The duration of each voltage pulse is  $3 \mu\text{s}$ .

rated (ADS) and the time during which the cells are addressed will be called the address period below. We discuss this driving method in Sec. IV.

The terminology generally used in the literature on PDPs is the following and will be used in the rest of this article. The first pulse in Fig. 2 is called “address pulse” or “data pulse” or “write pulse”. Specific voltages are applied between the scan electrode (scan write voltage) and address electrode (address voltage or data voltage) during this pulse. The following pulses in Fig. 2 are called sustain pulses and correspond to a square-wave voltage difference between the X and Y electrodes. The amplitude of this voltage must be less than the breakdown voltage between X and Y and its frequency will define the intensity of the light emitted by the display. The successive current pulses during sustaining and when the cell is ON are identical, and the eye does not distinguish the light emitted by each individual pulse. Note finally that a cell can also be turned ON by applying a large voltage pulse between the X and Y electrodes. Such a pulse is also called a write pulse in the literature on PDPs. In that case all the cells in a line are turned ON (i.e., there is no selectivity, as in the case of addressing with the scan and data electrodes; this write pulse is not an address pulse). This way of a turning the cells ON can be used in some particular driving methods (see Sec. V), and also to maintain a large enough background of charged particles in the display cells. In the latter case this operation is called priming. Its purpose is to prevent miswriting due to the lack of seed electrons when a cell must be addressed. Priming is applied at a low enough frequency to maintain a good contrast and must be followed by an erasing pulse. We do not discuss priming in this article.

## B. Address pulse

We consider here the first voltage pulse of Fig. 2. Figure 3 shows the potential contours and the power dissipated by electron into xenon excitation at three times during the address pulse (200, 214, and 222 ns). The voltage on the scan electrode Y is set to  $-200 \text{ V}$ , the X electrode voltage is set to  $0 \text{ V}$ , and the voltage on the data electrode A is at  $80 \text{ V}$ .

We see in the upper part of Fig. 3 that a discharge forms between the Y and A electrodes. The discharge formation and decay during the address pulse is similar to what we have described previously in the case of a matrix display.<sup>1</sup> The plasma first forms close to the dielectric surface above the anode (electrode A). It then expands towards the cathode (electrode Y), and an ion sheath forms and contracts above the dielectric surface on the cathode side. The maximum of power dissipated by electrons into xenon excitation is located at the interface between the sheath and the plasma (where the electron are still energetic and the electron flux is large). Local maximums of the power dissipated into electron excitation of xenon are also observed above the dielectric surface on the anode side, as in a matrix display.<sup>1</sup> The excitation in that region is due to the spreading of the plasma along the dielectric surface which is induced by a potential gradient along the surface resulting from the charging of the dielectric surface by electrons.

At the end of the address pulse positive and negative charges are present on the dielectric surfaces above the Y and A electrodes, respectively. These charges are going to make possible gas breakdown between the X and Y electrodes during the first sustain pulse described below.

## C. Sustain pulses

Although the voltage between the display electrodes (X and Y) is only  $180 \text{ V}$ , i.e., less than the breakdown voltage for this geometric configuration, a discharge is initiated between these two electrodes during the first sustain pulse. This is because, as can be seen in the lower part of Fig. 3, the voltage drop in the gas above the X and Y electrodes is on the order of  $300 \text{ V}$  due to the presence of the positive charges deposited by the address pulse on the dielectric surface above the Y electrode. The potential contours of Fig. 3 corresponding to the first sustain pulse show that the plasma first forms above the anode (which is now the Y electrode) and expands while a sheath forms above the cathode (X electrode). The data electrode does not play a significant role during this pulse, although, as we shall see in Sec. III C, a nonzero current is collected by the dielectric surface above the data electrode.

The evolution of the power dissipated by electrons into xenon excitation during the first sustain pulse (lower part of Fig. 3) shows that there are two maximums in the spatial distribution of the xenon excitation. One of the maximums of xenon excitation is located above the cathode and moves away from the gap between the display electrodes as the plasma expands. This maximum corresponds to the usual plasma sheath interface (negative glow). The second xenon excitation maximum is above the anode and corresponds to the spreading of the plasma along the surface above the anode which is induced, as in the case of the address pulse, by the potential gradient parallel to the surface and due to the charging of the surface by electrons. These two maximums of xenon excitation are correlated with the maximums of discharge emission (infrared and VUV) observed in experiments.<sup>12,13</sup> We do not observe under these conditions

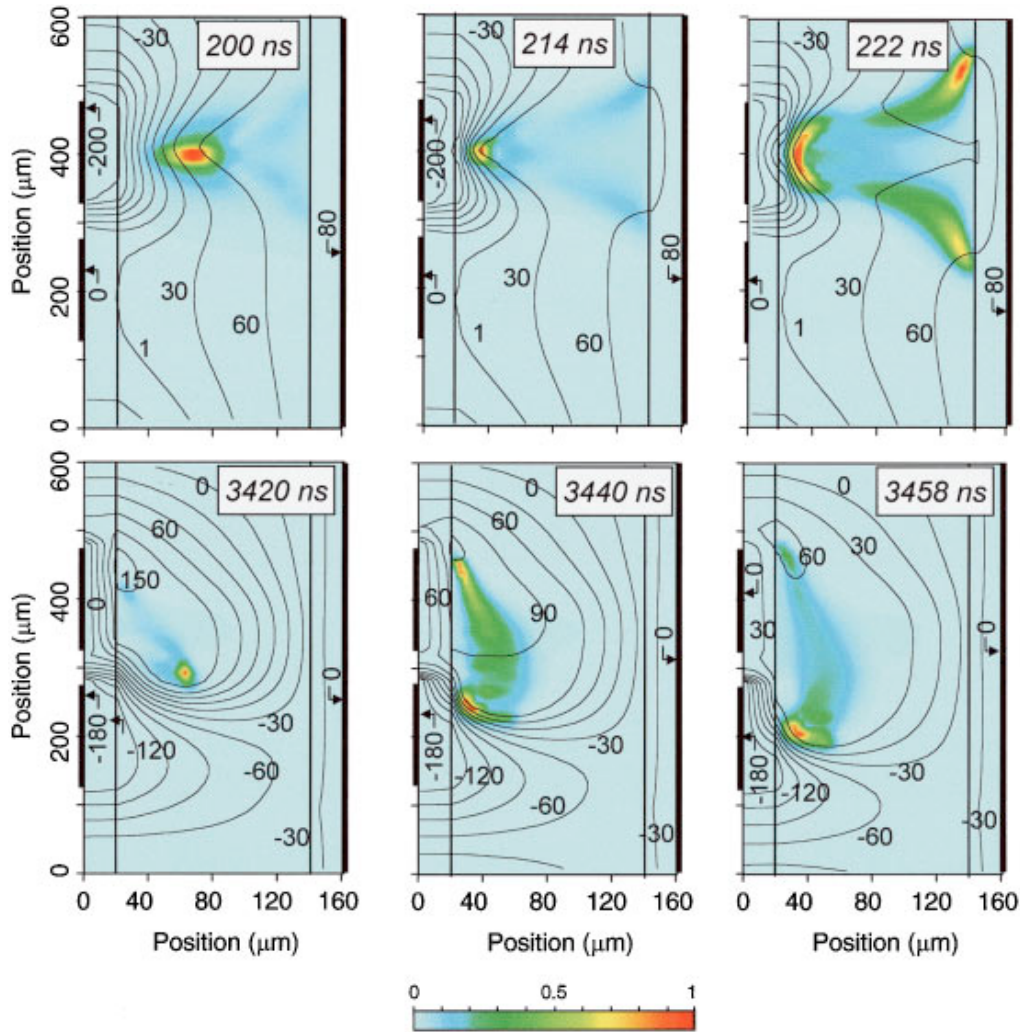


FIG. 3. Potential contours (lines), and power dissipated by electrons into xenon excitation (color contours) at three times during the address pulse (top) and at three times during the first sustain pulse (bottom). The unit for the power dissipated into xenon excitation is 4, 46, 22, 4.5, 42, 25  $\text{mW mm}^{-3}$  for times 200, 214, 222, 3420, 3440, 3458 ns, respectively. The gas mixture is Xe-Ne (5%-95%) at 500 Torr, the cell geometry is indicated in Fig. 1, and the driving voltages are those of Fig. 2.

the well structured striations above the anode, which have been seen in some experiments.<sup>12</sup>

#### D. Charge evolution on the dielectric layers

The current wave form and the time evolution of the charge density above the electrodes during the address and sustain pulses of Fig. 2 are shown in Figs. 4 and 5, respectively. For these conditions, the amplitude of the current through the Y and A electrodes during the address pulse is larger than the amplitude of the current flowing to the X and Y electrodes during the sustain regime. The duration of the current pulses is on the order of 100 ns for the first sustain pulse and about 50 ns for the address pulse. Figure 4(a) shows that there is practically no current to the X electrode during addressing and only a small current to the A electrode during the first sustain pulse. Figure 4(b) shows the time variations of the current to the electrodes during addressing

and for several subsequent sustaining cycles. It can be seen in Fig. 4(b) that a steady state is reached after a few sustain pulses.

The evolution of the charge density above the electrodes (Fig. 5) shows that most of the charges are deposited above the Y electrode (positive charges) and the A electrode (negative charges) during the write pulse. During the sustain regime, the negative charge above the data electrode A decreases during the first four or five pulses and reaches a value slightly less than the magnitude of the positive charge alternatively present above the X and Y electrodes. The charge above the coplanar electrode which is the instantaneous anode is negative but much smaller (in absolute value) than the charge above the data electrode A.

The charge on the surface of the dielectric above the X, Y, and A electrodes during the steady state sustain regime depends strongly on the cell geometry, on the value of the permittivity, and on the thickness of the dielectric layers above the display (X-Y) and data electrodes (A). This is

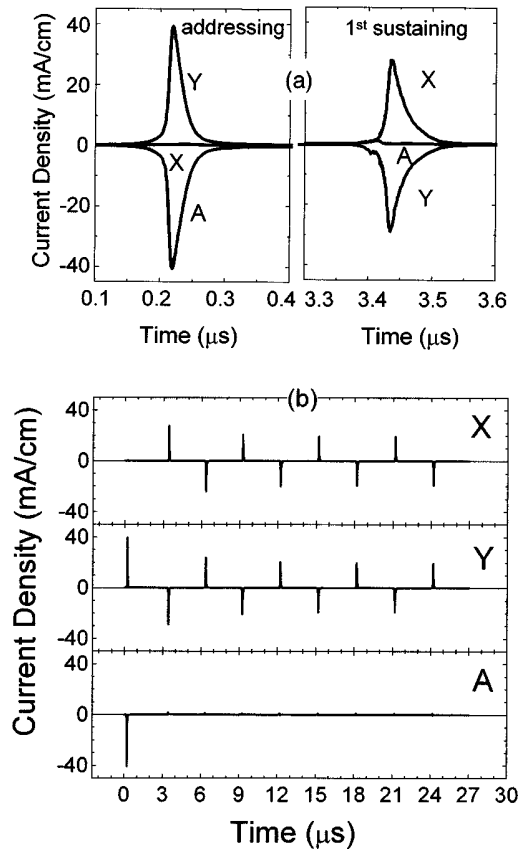


FIG. 4. Current density on each electrode during (a) the address pulse and the first sustain pulse, and (b) during a sequence including the address pulse and four sustaining cycles. Same conditions as Fig. 3.

illustrated in Fig. 6 which shows the time evolution of the charge density above the electrodes for the same geometry but for a permittivity of the dielectric layer above the data electrode equal to 3 instead of 10. The steady state value of the negative charge above the data electrode A for  $\epsilon=3$  is smaller than for  $\epsilon=10$  while the negative charge above the instantaneous anode (X or Y) is larger. Another factor which

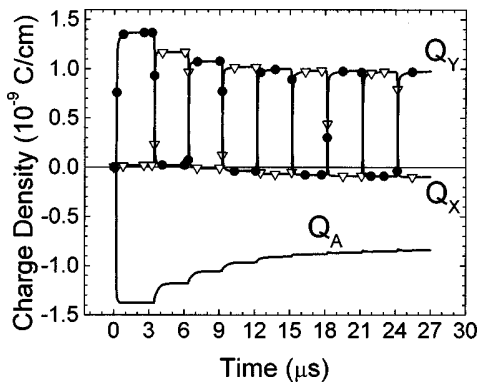


FIG. 5. Time evolution of the charge per unit length on the dielectric layer above each electrode in the conditions of Figs. 2–4.  $Q_X$  is the charge per unit length on the lower half of the dielectric surface above the display electrodes and  $Q_Y$  is the charge on the upper half of the surface above the display electrode.  $Q_A$  is the charge on the dielectric above the address electrode.

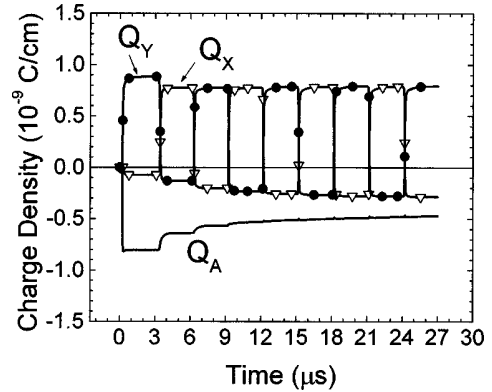


FIG. 6. Same as Fig. 5 for a relative permittivity of the dielectric layer above the address electrode equal to 3 instead of 10.

may affect the magnitude of surface charge above the three electrodes in the simulation is the 2D nature of the model; the data electrode A is actually a plane in the simulation, and it is clear that the capacitance of the dielectric layer above the data electrode is overestimated in the model.

#### IV. PRACTICAL DRIVING METHOD

We have seen in Sec. III the principles of addressing one individual cell, and we illustrated addressing and sustaining by using a simplified driving method. In practice a large number of cells must be addressed and one must carefully choose the time sequence of the voltage pulses applied to the different cells to address, sustain, and erase them. In Sec. IV we consider only the ADS method which has proved to be very efficient.<sup>14</sup> In this method the operation of addressing and sustaining are separated in time. The purpose of Sec. IV is to illustrate the existence of constraints on the values of voltage applied to the electrodes for proper addressing and to show the ability of the model to predict and help understand these constraints. Among the large variety of possible driving schemes using the ADS method we chose to study the scheme described by Nakamura *et al.* in Ref. 7.

We describe the principles of the chosen driving method in Sec. IV A. The constraints on the voltages applied to the electrodes during addressing and sustaining are described quantitatively with the help of the model in Sec. IV B.

##### A. Principles of the driving method and constraints

Figure 7 shows the voltage wave form applied to the electrodes for the driving method of Nakamura *et al.*<sup>7</sup> which is studied in Sec. IV A. The data electrode A defines a column of the display. A row of the display is defined by a couple of X-Y electrodes (display electrodes). All the X electrodes (sustain electrodes) have the same voltage. One can therefore describe the driving method by looking at the voltage applied to a given data electrode A, the common voltage of the X electrodes, and the voltage applied to each Y electrode. Figure 7 shows the voltage of one address electrode A, the X electrodes, and of two Y electrodes ( $Y_i$  and  $Y_j$ ). We see on this example that the cell defined by (A- $Y_i$ ) is first addressed. The (A- $Y_j$ ) is addressed at a later time. This driving scheme uses the ADS method and all the cells are first

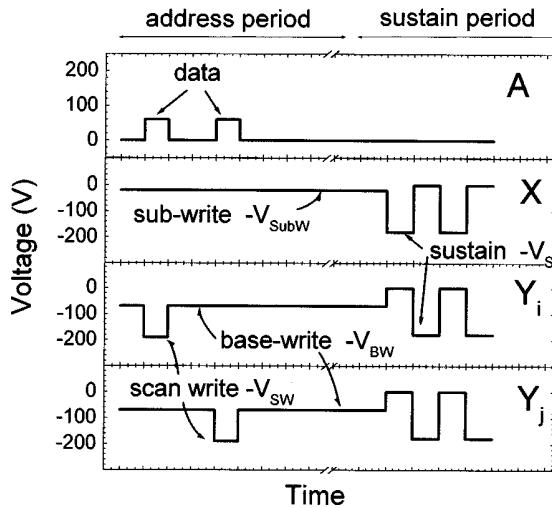


FIG. 7. Example of driving voltages described in Ref. 7 and used in Sec. IV.  $Y_i$  and  $Y_j$  are two different lines sharing the same data electrode A. The voltage of the X sustain electrodes associated with  $Y_i$  and  $Y_j$  are identical. An address pulse is first applied between  $Y_i$  and A, and then between  $Y_j$  and A.

addressed line by line during the address period which lasts for a few hundred microseconds ( $3 \mu\text{s}$  per line in the conditions of Ref. 15). Addressing of a given cell is done by applying a data voltage to the A electrode and a scan write voltage to the Y electrode. The scan write voltage pulses are applied sequentially to all the Y electrodes. The data voltage is applied only to those cells which are selected. Once a cell has been addressed, its state must not be changed during the time the other cells along the same data electrode are addressed, i.e., until sustaining starts. The sustain period can start after all the cells have been addressed.

Two important features must be considered for successful addressing: (1) after a cell (A- $Y_i$ ) has been addressed the voltage drop between  $Y_i$  and A must be such that no more discharging occurs between Y and A before sustaining starts, and (2), since the data electrode is shared by all the line electrodes, the voltages applied to the data electrode must not initiate a discharge in a nonselected cell. The first point means that the values of the voltage applied to electrodes of a cell after this cell has been addressed must be chosen carefully in order to prevent a cancellation of the memory charges deposited by the address pulse. The total or partial cancellation of these memory charges may put the cell back in the OFF state. This is called self-erasing. Suppose for example that after the address pulse for a given cell, the three electrodes are put to a zero voltage. If the memory charges deposited by the address pulse above the Y and A electrodes are large enough, the voltage drop between the dielectric surfaces above Y and A may become sufficient to initiate a discharge (self-erasing discharge).

In order to avoid self-erasing the voltages applied to the electrodes of a cell during the addressing of the other cells and before the sustain period can be chosen as in Fig. 7. Applying a nonzero, negative voltage to the scan electrode (Y electrode) after writing prevents self-erasing because it decreases the voltage drop in the gap between the dielectric

surfaces above Y and A (this voltage drop is related to the difference between the voltage drop across the dielectric layers due to the memory charges, and the voltage drop between the A and Y electrodes). The nonzero voltage applied to Y is called the base-write voltage by Nakamura *et al.*<sup>7</sup> The voltage applied to the scan electrode in order to put a cell in the ON state is called the scan write voltage. A nonzero voltage can also be applied to the sustain electrode X during the address period as described in Ref. 7. This voltage is called the subwrite voltage in Ref. 7. These different voltages are indicated in Fig. 7. Finally the data voltage and base-write voltage must be chosen in such a way that a cell cannot be turned to the ON state because of the voltage drop between the Y and A electrodes induced by the base-write and data voltages alone.

There are also some constraints on the voltage applied to the X and Y electrode during sustaining. This voltage must be obviously lower than the breakdown voltage between X and Y (otherwise the cells could not be turned to the OFF state), yet it must be large enough to maintain the cell ON during the successive sustain pulses.

The discussion above shows that the voltages applied to the electrodes during addressing and sustaining must be within limits. These limits define the "voltage margins" of the display. The voltage margins of the driving method of Fig. 7 are derived below with the help of the 2D model. A discussion of the voltage margins in the simpler case of a matrix display can be found in Meunier, Belenguer, and Boeuf,<sup>3</sup> and references therein.

## B. Voltage margins

In the driving method of Fig. 7 a cell is turned to the ON state when a data pulse is applied to the A electrode while a scan write pulse is applied to the Y electrode. The scan write voltage is applied successively to all the Y electrodes along the length of a data electrode. The data voltage is applied, simultaneously to the scan write voltage, selectively to those cells which must be turned to the ON state. The voltage drop between Y and A when the cell is addressed is ( $V_{SW} + V_D$ ). For a given  $V_{SW}$ , addressing is successful only if  $V_D$  is larger than a lower limit. There is also an upper limit of  $V_D$  because if  $V_D$  is too large it is possible, as mentioned above, that (1) self-erasing partly erases the charges deposited during writing of the cell, or (2) that other cells sharing the same data electrode (i.e., on the same column) are affected by the data pulse applied to turn on a particular cell. These lower and upper limits of the data pulse voltage define the margin of the data pulse voltage.

The sustain voltage of the cell (applied between X and Y electrode during the sustain period) must also be within limits in order to allow selective writing and erasing of the cells. The voltage margins of the data and sustain voltages are described below, and comparisons between calculations and measurements are presented.

### 1. Data pulse voltage margin

From the discussions above it is clear that depending on the value of the base-write voltage, and for a given value of the scan write voltage, the data voltage must be below an

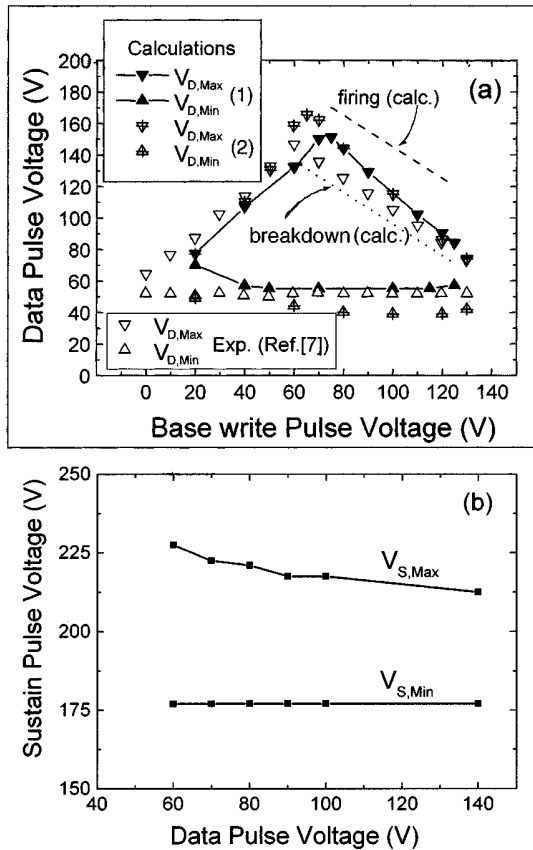


FIG. 8. (a) Calculated and measured (see Ref. 7) minimum and maximum data pulse voltage as a function of base-write voltage for the driving method of Fig. 8 with a scan write voltage of  $-190$  V and a subwrite voltage of  $-20$  V. The full black triangle [case (1)] corresponds to the calculations for the geometry and gas mixture as in Fig. 3 (this geometry is close to the geometry of a cell in a 20 in. diagonal PDP). The triangles with a center cross [case (2)] correspond to a similar cell but with a  $90 \mu\text{m}$  gap between coplanar electrodes, instead of  $50 \mu\text{m}$  (geometry closer to a 40 in. diagonal PDP). The calculated firing and breakdown voltages correspond to case (1). The measurements correspond to a 40 in. ac coplanar PDP (see Ref. 7); (b) Calculated minimum and maximum sustain voltage as a function of the data pulse voltage for the driving method of Fig. 7. Geometry and gas mixture as in Fig. 3.

upper limit if one wants to prevent an unsuccessful writing due to self-erasing. This is illustrated in Fig. 8(a) where the calculated (and measured) minimum and maximum values of the data pulse voltage are plotted as a function of the base-write voltage, for the cell described above and for the driving sequence of Fig. 7 with a scan write voltage ( $-V_{SW}$ ) of  $-190$  V. and a subwrite pulse ( $-V_{SubW}$ ) of  $-20$  V. We see in Fig. 8(a) that the upper limit of the data pulse  $V_D$  increases when the base-write voltage  $V_{BW}$  is larger. This is because self-erasing cannot occur, even for large data pulse voltages, if  $V_{BW}$  is large enough. However above a given value of  $V_{BW}$  [about  $70$  V in the conditions of Fig. 8(a)] the upper limit of the data pulse voltage starts to decrease with increasing  $V_{BW}$ . The existence of the upper limit of the data pulse voltage in this region is no longer due to self-erasing problems, but it is rather due to the requirement that the state of nonselected cells along the same column (same data electrode) must not be affected when a selected cell is turned in the ON state (i.e., when the data pulse is applied to turn this

cell on). When the cell corresponding to the  $Y_i$  scan electrode is addressed in Fig. 7 (first data pulse) the cell defined by  $Y_j$  and A should not be turned ON. This cell, and all the cells along the same column “see” a voltage equal to  $(V_{BW} + V_D)$  between scan and data electrodes. This voltage must be lower than the firing voltage, the minimum voltage which must be applied between scan and data electrodes to turn the cell in the ON state, and hence to initiate a sequence of discharge pulses between X and Y electrodes during the sustain period. The value of  $(V_{BW} + V_D)$  corresponding to the firing voltage is indicated by a dashed line in Fig. 8(a). If the value of  $(V_{BW} + V_D)$  is less than the breakdown voltage between scan and address electrode then nonselected cells will not be disturbed when a cell is turned in the ON state by the combination of a scan pulse and a data pulse. The value of  $(V_{BW} + V_D)$  corresponding to the breakdown voltage between facing electrodes Y and A is indicated by a dotted line in Fig. 8(a). If  $(V_{BW} + V_D)$  is larger than the breakdown voltage of the Y and A electrodes [ $\sim 196$  V in the conditions of Fig. 8(a)], but lower than the firing voltage ( $\sim 245$  V), it is still possible to have addressing problems. This is because even if the firing of an unselected cell does not happen, a non-negligible charge transfer between Y and A can occur if  $(V_{BW} + V_D)$  is larger than the breakdown voltage between Y and A. If the charge transfer between  $Y_j$  and A during the addressing of the  $(Y_j-A)$  cell is too large it will not be possible to turn the  $(Y_j-A)$  cell ON when necessary [see for example the second data pulse in Fig. 8(a) which is aimed at turning this cell in the ON state]. One can therefore conclude that, for a given scan write voltage and a given base-write voltage, the upper limit of the data pulse voltage must be such that  $(V_{BW} + V_D)$  is somewhere between the breakdown voltage and the firing voltage. We have calculated this upper limit by looking for the maximum data pulse voltage which can be applied to a cell without preventing another cell to successfully be turned on at a subsequent time. The result is the full line in Fig. 8(a) between the breakdown voltage line (dotted line) and the firing voltage line (dashed line).

The lower limit of the data pulse voltage is also represented in Fig. 8(a). This lower limit corresponds to the minimum value of the voltage between Y and A ( $V_{BW} + V_D$ ), leading to successful firing of the cell when the scan write voltage is applied to Y and the data voltage is applied to A. This means that addressing occurs only if enough charges are deposited on the dielectric surfaces above Y to ensure steady state sustaining between X and Y during the sustain period. This minimum value of  $(V_{SW} + V_D)$  is equal to  $245$  V in the conditions of Fig. 8(a). Since  $V_{SW}$  is kept constant and equal to  $190$  V in Fig. 8(a), this corresponds to a lower limit of  $V_D$  of about  $55$  V (this value slightly increases when  $V_{BW}$  is small).

The variations of the calculated upper and lower limits of the data pulse as a function of the base write pulse in Fig. 8(a) are in excellent agreement with the experimental results of Nakamura *et al.*<sup>7</sup> The calculations shown in Fig. 8(a) correspond to two different cells. The first case [full triangle symbols, noted (1)] correspond to the cell described above (conditions close to a 20 in. diagonal PDP, with a  $50 \mu\text{m}$  gap between the coplanar electrodes and  $120 \mu\text{m}$  gas gap be-

tween the two plates). The second set of calculations (triangles with center cross) correspond to conditions closer to a 40 in. display (90  $\mu\text{m}$  gap between coplanar electrodes and 120  $\mu\text{m}$  gap between the two plates). Note that the differences between the two different cells are not very large. This is because the minimum and maximum voltages of Fig. 8(a) depend mainly on the gas gap (120  $\mu\text{m}$  in both cases), and much less on the coplanar electrode gap or electrode width (which would be different in 20 and 40 in. PDPs).

**2. Sustain voltage margin**

The sustain voltage must also be within a finite interval called the sustain voltage margin. The upper limit of this voltage is equal to the breakdown voltage between the two coplanar electrodes and sustaining is impossible below the lower limit of the sustain voltage. Figure 8(b) shows the variations of the minimum and maximum sustain voltages as a function of the data pulse voltage in the same conditions as above, for a base-write voltage of  $-60\text{ V}$  and for a subwrite voltage of  $-20\text{ V}$ . For this value of  $V_{BW}$ , the data voltage margin is close to its maximum [see Fig. 8(a)]. The sustain voltage margin is on the order of  $50\text{ V}$  in the conditions of Fig. 8(b). We also see that the maximum sustain voltage slightly decreases with increasing data pulse voltage. This is because when the data voltage increases it is possible that a small charge transfer occurs between Y and A electrodes even for nonselected cells (see above). This charge transfer induces a voltage on the surface of the dielectric layers which lowers the breakdown voltage between the sustain electrodes X and Y.

**V. OTHER ADDRESSING METHODS**

In Sec. IV we have described one particular driving method. Due to the presence of three electrodes in a coplanar display cell, different driving methods are possible. In the examples above the sustain voltage is negative with respect to the voltage applied to the data electrode during the sustain period. In some driving methods<sup>15</sup> the sustain voltage is positive with respect to the voltage on the data electrode during sustaining. The charge on the surface above the data electrode during sustaining must therefore be positive, in contrast to the case described above and the sequence of voltages which must be applied to the electrodes in order to turn a cell to the ON state is different from the case above.

Shinoda *et al.*<sup>6</sup> have described a particular driving method where all the cells in a line are first turned in the ON state (i.e., a write pulse is applied to all the cells during the write period). The unselected cells are then erased during the address period. This method is called erase addressing and is illustrated in Fig. 9. The scan write pulse (see Fig. 9) is applied only to those cells which are not selected, i.e., which must be put in the OFF state. The driving method of Fig. 9 has been simulated with our 2D model and Fig. 10 shows the calculated time evolution of the currents and charge per unit length above each electrode for these conditions (same geometry as above, gas mixture with 3% xenon in neon). The time evolution of the currents and charges show that there is no more current or charge transfer after pulse number 6

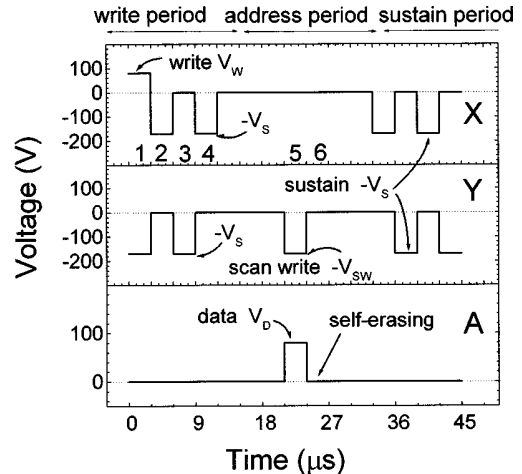


FIG. 9. Driving voltages used to simulate the erase-addressing method. The sustain voltage  $V_s$  is  $170\text{ V}$ , the data voltage  $V_d$  is  $80\text{ V}$ , and the scan write voltage  $V_{sw}$  is also equal to  $-170\text{ V}$ .

which indicates that the cell has been successfully turned off. If the scan pulse is not applied, the calculations (not presented here) show that the cell stays in the ON state, i.e., a current pulse is observed between the scan and sustain electrodes at each pulse of the sustain period. It appears in Fig. 10 that the cell is turned off during the discharge pulse (#6)

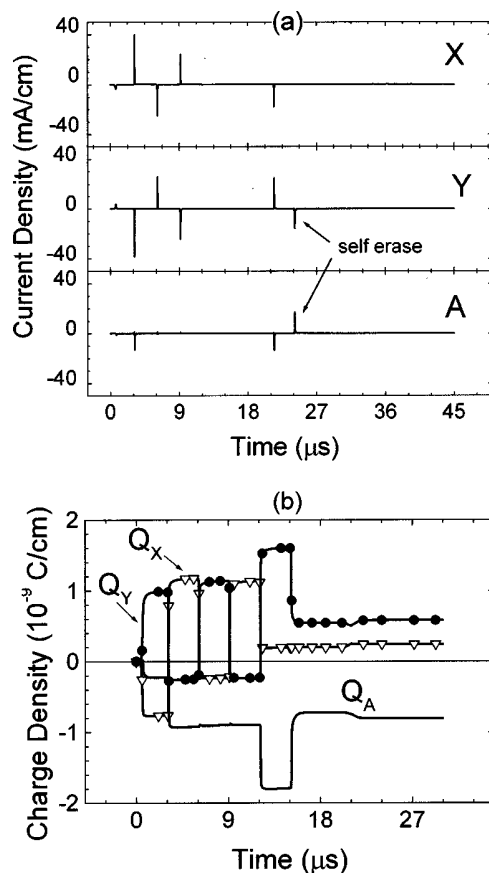


FIG. 10. Time evolution of (a) the calculated current to each electrode, and (b) the charge per unit length above each electrode for the erase-addressing method of Fig. 9. Same geometry as in Fig. 3, gas mixture 3% Xe in Ne.

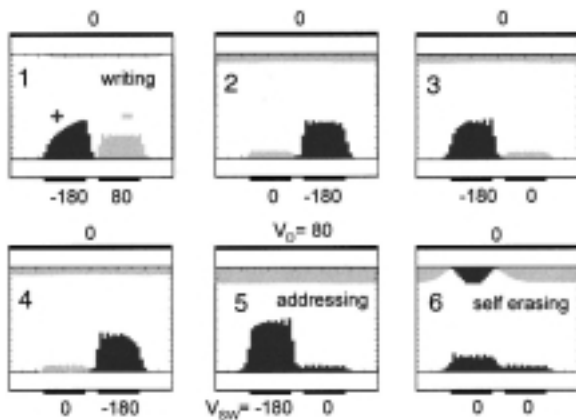


FIG. 11. Charge distribution above the dielectric layers at the end of each discharge pulse for the driving method of Fig. 9. The numbers refer to the pulse numbers of Fig. 9. The darker areas correspond to positive ions and the lighter areas correspond to electrons. The unit of the charge density is the same for all the curves.

occurring immediately after the data and scan pulse (#5) are applied to the cell. The voltages on the electrodes during pulse #6 are zero, and the discharge occurring between the Y and A electrode during that pulse is similar to a self-erasing discharge as described in Sec. IV.

The charge distribution above the electrodes after each discharge pulse are represented in Fig. 11. We see that the first pulse creates a discharge between the sustain electrodes X and Y. After the second pulse the dielectric above the X electrodes is positively charged while the dielectric layers above the Y and A electrodes are covered with negative charges. Most of the negative charges are however above the data electrode in the conditions of Fig. 11, and at the end of pulses 2, 3, and 4. The discharges of pulses 2, 3, and 4 are similar and this regime looks like a steady state sustain regime. During the address pulse (pulse #5) the data electrode collects an electron current and an excess of positive charges is deposited above the Y electrode. The charges above the Y and A electrodes at the end the address pulse 5 are so large that when the electrode voltages are set to zero again (pulse #6) the voltage drop induced by these charges is sufficient to initiate a discharge between Y and A which cancels a large part of the charges previously deposited above Y and A. This discharge is therefore similar to the self-erasing discharge describe in Sec. III. We see that although the cancellation of the charges during the self-erasing discharge #6 is sufficient to prevent reignition of the cell during the sustain period, there is still a non-negligible amount of charges above the dielectric layers after the cell has been turned off. The amount of remaining charges is obviously related to the exact value of the scan write and data voltages, and it is clear that one could define a margin for these voltage pulses. We will not present here a systematic study of the margins for this driving method.

## VI. CONCLUSION

A 2D discharge model has been developed and used to study different driving methods of coplanar plasma display

panels. The physical model is similar to the one described in Ref. 1 and the numerical method has been improved to allow fast simulation of successive discharge pulses (semi-implicit method of integration of transport equations coupled with Poisson's equation).

The driving method of Nakamura *et al.*<sup>7</sup> which is used in mass-produced PDPs has been successfully simulated. The space and time evolution of the plasma shows a spreading of the plasma electrons along the dielectric surfaces accompanied with an increase in electron impact excitation of xenon, in qualitative agreement with the experimental observations. The properties of the calculated voltage margins are in excellent qualitative agreement with the experimental measurements. The model provides a clear qualitative and quantitative explanation of the variations of the voltage margins with the discharge and driving voltage parameters.

Another driving method where addressing is used to erase unselected cells has also been simulated. The ability of the models to reproduce different driving methods makes it a very useful tool for the understanding and improvement of PDPs.

## ACKNOWLEDGMENTS

This work is partially supported by Thomson Plasma. The numerical model used in this work has been developed in collaboration with Kinema Software. The authors would like to thank L. C. Pitchford for carefully reading the manuscript and for a number of suggestions and comments.

- <sup>1</sup>C. Punset, J. P. Boeuf, and L. C. Pitchford, *J. Appl. Phys.* **83**, 1884 (1998).
- <sup>2</sup>J. P. Boeuf, C. Punset, A. Hirech, and H. Doyeux, *J. Phys. IV* **7**, C4-3 (1997).
- <sup>3</sup>J. Meunier, P. Belenguer, and J. P. Boeuf, *J. Appl. Phys.* **78**, 731 (1995).
- <sup>4</sup>R. Veerasingam, R. B. Campbell, and R. T. McGrath, *IEEE Trans. Plasma Sci.* **24**, 1399 (1996).
- <sup>5</sup>Y. Sano, T. Okajima, N. Koyama, T. Yoshioka, and K. Nunomura, *SID'91 Digest*, 1991, p. 728.
- <sup>6</sup>T. Shinoda, M. Wakitani, T. Nanto, T. Kurai, N. Awaji, and M. Suzuki, *SID'91 Digest*, 1991, p. 724.
- <sup>7</sup>T. Nakamura, K. Iseki, Y. Sano, and K. Nunomura, *SID'95 Digest*, 1995, p. 807.
- <sup>8</sup>H. Hirakawa, T. Katayama, S. Kuroki, T. Kanae, H. Nakahara, T. Nanto, Y. Yoshikawa, A. Otsuka, and M. Wakitani, *SID'98 Digest*, 1998, p. 279.
- <sup>9</sup>H. K. Gummel, *IEEE Trans. Electron Devices* **ED-11**, 455 (1964); D. L. Scharfetter and H. K. Gummel, *ibid.* **ED-16**, 64 (1969).
- <sup>10</sup>P. L. G. Ventzek, R. J. Hoekstra, and M. J. Kushner, *J. Vac. Sci. Technol. B* **12**, 461 (1994).
- <sup>11</sup>J. P. Boeuf, Th. Callegari, R. Ganter, and C. Punset, *Asia Display'98*, 1998, p. 209.
- <sup>12</sup>H. Uchiike, *Workshop Digest of Technical Papers, ASIA Display'98*, 1998, p. 195; M. Sawa, H. Uchiike, S. Zhang, and K. Yoshida, *SID'98 Digest*, 1998, p. 361.
- <sup>13</sup>K. W. Whang, H. S. Jeong, J. H. See, C. K. Yoon, and J. K. Kim, *IDW'97*, 1997, pp. 531-534.
- <sup>14</sup>S. Kanagu, Y. Kanazawa, T. Shinoda, K. Yoshikawa, and T. Nanto, *SID'92 Digest*, 1992, p. 713.
- <sup>15</sup>K. Yoshikawa, Y. Kanazawa, M. Wakitani, T. Sinoda, and A. Ohtsuka, *Japan Display'92 Digest*, 1992, p. 605.